Rheol Acta (2006) 46: 33–44
DOI 10.1007/s00397-005-0065-z

ORIGINAL CONTRIBUTION

Masataka Sugimoto
Yasuhiro Suzuki
Kyu Hyun
Kyung Hyun Ahn
Tsutomu Ushioda
Akihiro Nishioka
Takashi Taniguchi
Kiyohito Koyama

Melt rheology of long-chain-branched polypropylenes

Received: 16 October 2005
Accepted: 26 October 2005
Published online: 21 December 2005

M. Sugimoto · Y. Suzuki · A. Nishioka · T. Taniguchi · K. Koyama (✉)
Department of Materials Science and Engineering,
Yamagata University,
4-3-16 Jonan,
Yonezawa, 992-8510, Japan
e-mail: koyama@yz.yamagata-u.ac.jp

K. Hyun · K. Hyun Ahn
School of Chemical Engineering,
Seoul National University,
San 56-1 Shillim-dong, Gwanak-gu,
Seoul, 151-744, South Korea

T. Ushioda
Polymerization Technical Center,
Japan Polypropylene Corporation,
1 Toho-cho,Yokkaichi,
Mie, 510-0848, Japan

Abstract Rheological properties of long-chain-branched isotactic polypropylene (PP) via copolymerization with a very small amount of nonconjugated α,ω-diene monomer using metallocene catalyst system in both linear and nonlinear regions were investigated, comparing with conventional linear and long-chain-branched PP modified at postreactor. Although comonomer incorporation was equal to 0.05 mol% or less, it caused high molecular weight, broad molecular weight distribution, and long-chain branching. A detailed study on the effect of diene incorporation on the polymer properties was conducted, comparing with modified PP in postreactor. Polymer chain microstructures were characterized by gel permeation chromatography with multiangle laser light scattering (MALLS), differential scanning calorimetry, and rheological means: dynamic viscoelasticity, step-strain, uniaxial elongational flow measurements, and large amplitude oscillatory shear. The PP, which incorporated a small amount of diene monomer, showed significantly improved viscoelastic behaviors. The diene-propylene copolymer containing long-chain branches showed extremely long relaxation mode under shear and outstanding viscosity increase under elongational flow, so-called strain hardening. The difference in microstructure of diene-propylene copolymer with modified PP with long-chain branches is investigated by MALLS and rheological characterizations.

Keywords Diene-propylene copolymer · MALLS · Long-chain branch · Strain hardening · Step-shear stress relaxation · LAOS

Introduction

Polypropylene (PP) is one of the most globally produced and widely used polymers in the marketplace since PP has good physical properties such as rigidity, impact strength and chemical resistance, and a low cost. The processability of PP is often unfavorable, as the melt strength of PP is low in comparison with those of polyethylenes (PEs). Therefore, considerable efforts were made to improve the melt rheological properties of PP (Gotsis and Zeevenhoven 2004; Hingmann and Marczinke 1994; Scheve et al. 1990; Sugimoto et al. 1999, 2001a,b; Weng et al. 2002; Williams et al. 1998; Wong and Baker 1997; Yoshii et al. 1996).

Long-chain-branched, moderately cross-linked or highly branched polymers were found to have the following rheological properties: lower Newtonian viscosity and strong shear thinning at same molecular weight, strong melt elasticity expressed by the first normal stress difference and storage modulus, and enhanced strain hardening under elongational flow. As for PP, numerous reports have illustrated that chemical treatment enables a production of long-chain branches. Electron beam irradiation causes chain-scission and polymer degradation but could also lead to improved melt rheology (Scheve et al. 1990; Sugimoto et al. 1999; Williams et al. 1998; Yoshii et al. 1996). The combination of electron beam with polyfunc-

tional monomers was found to enhance elasticity and strain hardening (Yoshii et al. 1996). Several approaches using peroxides have been explored to improve the processability of PP (Hingmann and Marczinke 1994; Sugimoto et al. 1999; Tsenoglou and Gotsis 2001; Wong and Baker 1997). A peroxide initiator has been used to promote free-radical melt grafting of functional monomers onto the polymer molecules. Some organic peroxides, which decompose at low temperature, are used to promote branching reaction because of the high reactive efficiency and dehydrogenation ability from polymer chains. Unfavorable effects of these postreactor treatments may be residues and odor due to uncontrolled decomposing reaction.

In this study, we used metallocene-catalyzed propylene-diene copolymer with a very small amount of nonconjugated diene. The homogeneous single-site catalysts not only enable the production of polyolefins with narrow molecular weight distribution, narrow chemical composition distribution, and precisely controlled stereoregularity of polymer chain, but also allow the copolymerization with higher olefins and long-chain branching by incorporating added vinyl-ended or in situ generated macromonomers (Paavola et al. 2004; Weng et al. 2002; Ye et al. 2004). The methodology of copolymerization of propylene with diene in this study is important as an in situ polymerization of long-chain-branched PP in reactor. It has been known that a very small amount of diene causes a significant level of long-chain branches (Paavola et al. 2004; Ye et al. 2004). As for PE, Gabriel et al. (2002) reported molecular characterization with gel permeation chromatography (GPC) with multiangle laser light scattering (MALLS) and nuclear magnetic resonance (NMR), and rheological characterization for metallocene-catalyzed ethylene homopolymers. Some studies have been reported on copolymerization of ethylene with nonconjugated α,ω-dienes by using metallocene catalyst (Kokko et al. 2001). These studies focus on the synthesis of α-olefin with nonconjugated dienes. Few detailed studies have so far been made on rheology and structure of propylene copolymer incorporated with nonconjugated α,ω-dienes by metallocene catalysis. On the other hand, some studies for long-chain-branched PP modified in a postreactor have been examined from the viewpoint of melt rheology. However, difference of the physical properties and microstructure between metallocene catalyzed and modified polymer is still open to question. In this study, we report the fundamental study on the rheological properties and characterization of microstructure of PP incorporated with a small amount of 1,9-decadiene. The data obtained were compared with those of conventional PP and long-chain-branched PP treated by high-energy electron beam irradiation at postreactor. We performed rheological analysis by dynamic shear, step-shear and elongational viscosity tests. Furthermore, large amplitude oscillatory shear (LAOS) measurements in nonlinear regime were carried out to characterize and discuss the relationship between their rheological behaviors and difference of the microstructure of propylene-nonconjugated diene copolymer. This analysis has an importance in characterizing the flow of polymer melts since a polymer solution or melt undergoes large strain in actual polymer processing operation. Nonlinear response is frequently measured in the steady-state nonlinear regime. It has been reported that the LAOS test can provide plentiful additional information on the microstructure in the nonlinear regime (Yosick et al. 1997). In this article, we apply large oscillatory shear strain to complex polymer samples. Although there have been many works on the LAOS, only few attempts were made with long-chain-branched polymers.

Experimental

Materials

Three grades of PPs were used: PP-A, PP-B, and PP-C. PP-A is a commercial grade of Chisso Corporation or Japan Polypropylene Corporation (Grade: K1014); PP-B is a copolymer of propylene and a very small amount of 1,9-decadiene, which was produced at 0.05 mol% 1,9-decadiene monomer concentration using the supported metallocene catalyst activated with methylamuminoxane. The detailed polymerization procedure is described elsewhere (Tsutsui et al. 2001). The actual diene content used for the copolymer incorporation could not be detected by NMR (13C NMR, GX270, Jeol) due to the detection sensitivity limit. The desired metallocene homo PP was not obtained without the diene component under the same reaction conditions as PP-B, resulting in very high melt flow rate (MFR; >100 g/10 min) and low molecular weight. Reactor powder incorporated with phenol-type stabilizer was palletized by a single-screw extruder. The other sample (PP-C) is a propylene homopolymer treated with electron beam irradiation at postreactor that contains long-chain branches according to the manufacture.

Gel permeation chromatography with multiangle laser light scattering

A presence of branch causes classical gel permeation chromatography (GPC) to fail in measuring accurate molecular weight since difference in molecular conformation strongly affects the hydrodynamic volume. The average molecular weight, molecular weight distribution, and branching degree were determined by GPC coupled to an online multiangle laser light scattering (GPC-MALLS) system. GPC-MALLS measurements are not affected by the hydrodynamic volume because absolute molar masses are obtained with the light scattering technique.

In the size exclusion and MALLS measurements, samples were dissolved in 1,2,4-trichlorobenzene. The samples

were injected into Waters 150 chromatograph operating at 135°C, at a flow rate of 1.0 mL/min. The detection system was composed of 14 photodetectors placed at precise angles around the sample cell to collect and analyze the scattered laser light. The wavelength of the laser light source was 690 nm. The GPC-MALLS results were analyzed by commercial software ASTRA (Wyatt Technology Co.).

Differential scanning calorimetry

Differential scanning calorimetry (DSC) analyses were performed by a PerkinElmer Model DSC-7. The measurements were carried out at a heating rate of 20°C/min under dry nitrogen atmosphere. A sample of 10 mg was used. To remove the thermal history, the sample cell was heated from the room temperature to 230°C and then cooled to −20°C. For the melting test, a second run was made at a heating rate of 20°C up to 230°C, immediately after the first run was completed. The melting temperatures reported here were obtained from the second melting endotherm.

Viscoelastic measurements

Dynamic test

Shear dynamic measurements were carried out on a rheometer (Ares, TA instruments) using parallel plates with a diameter of 25 mm. The gap height of the plates was about 2 mm for the frequency sweeps. The samples were prepared by compression molding at 200°C, followed by cut from the sheet. The frequency range was 0.3–100 rad/s, and the maximum strain was fixed at 5%. We confirmed that these conditions were within the linear viscoelastic region. The temperature was kept constant at 180°C, and dry nitrogen was maintained to suppress oxidative degradation of the samples during the experiments.

The time sweeps were conducted at a frequency of 0.1 rad/s, the maximum strain of 5%, and the temperature of 180°C, to confirm a change in the molecular structure of the samples.

Step-shear stress relaxation

Stress relaxation measurements were performed by Ares (TA Instrument). Parallel plates of 25 mm in diameter and of 1 mm in the gap height were used for PP-A and PP-C. The shear relaxation moduli were corrected owing to the inhomogeneity of strain in the plates (Soskey and Winter 1984). For PP-B, we used cone-and-plate (25-mm plate diameter and cone angle of 0.1 rad) configuration, as the parallel plate correction was not applicable for PP-B. Therefore, the step-shear experiments of PP-B were conducted with more attention to slippage between plate and sample. The relaxational stresses $\sigma(t, \gamma)$ were measured over three decades of magnitudes after imposition of step strain γ(=0.3–6 for PP-A and PP-C, 0.1–5 for PP-B) at 180°C, and the nonlinear relaxation moduli $G(t, \gamma)$ were determined using the expression:

$$G(t, \gamma) = \sigma(t, \gamma)/\gamma$$

The data before the step strains were imposed were excluded.

Uniaxial elongational viscosity

For elongational viscosity measurements, the samples were prepared by compression molding at 200°C into the sheet shape of 1- to 2-mm thickness. The test specimens were cut in a width of 10 mm and the length of 56 mm. The sample width was recorded during the tests to confirm the uniform elongation and to calculate the actual strain rates. The measurements were carried out at constant strain rates of 0.05–1 s^{-1} and temperature of 180°C. The test chamber was maintained by dry nitrogen to suppress oxidative degradation of the samples.

LAOS measurement

Nonlinear oscillatory measurements were carried out on a strain-controlled rheometer (RMS 800, TA Instrument) using a parallel plate fixture with a diameter of 25 mm. For the raw data acquisition, a 16-bit ADC card (PCI-6052E; National Instruments, Austin, USA) with a sampling rate up to 333 kHz was used. This ADC card was plugged into a stand-alone PC equipped with LabView software (National Instruments). Strain sweep tests were carried out in the strain range from 10 to 1,000% at a fixed frequency of 1 rad/s and constant temperature of 180°C. The stress data were obtained simultaneously by ADC card.

Results and discussion

DSC and GPC-MALLS analysis

The molecular characterization was carried out by multi-angle laser light scattering analysis coupled with a GPC instrument (GPC-MALLS), which gives molecular weight and the radius of gyration (R_g) for the eluted polymer fractions from the GPC column. The absolute molecular weight was determined by laser light scattering at each retention volume, and the R_g was obtained by fitting the angular dependence of the light scattering signal to a random coil model for both linear and branching molecules.

Molecular weight distribution curves for the linear PP-A, and PP-B, and PP-C are given in Fig. 1. PP-A shows a single peak and mono-modal molecular weight distribution. Table 1 shows the number-average, weight-average and molecular distribution, $\overline{M}_n$, $\overline{M}_w$ and $\overline{M}_w/\overline{M}_n$, respectively, measured by GPC-MALLS. PP-B has low molecular weight and similar distribution shape in comparison with PP-A, though it has a slight tail in high molecular weight region. PP-C clearly shows a shoulder in the high molecular weight region of the curve.

In the θ solvent, the ratio of the mean square gyration radius of branching polymer $\left\langle R_g^2 \right\rangle_b$ to that of linear polymer $\left\langle R_g^2 \right\rangle_l$ (at same molecular weight) was represented by g known as Zimm-Stockmayers branching parameter g (Zimm and Stockmayer 1949):

$$g = \left\langle R_g^2 \right\rangle_b \Big/ \left\langle R_g^2 \right\rangle_l \tag{1}$$

The radius of gyration depends on the molecular architectures: a g parameter smaller than unity indicates a presence of branching chains. Fig. 2 shows the double-logarithm plot of radius of gyration R_g vs molecular weight M for PP-A, PP-B, and PP-C. The values of R_g of PP-B and PP-C are apparently lower than that of linear PP-A. This plot provides information concerning the conformation of polymer chains in the 1,2,4-trichrolobenzene solutions. For these samples, the relationship between R_g and M is well described by power law:

$$R_g = kM^{\alpha} \tag{2}$$

The slopes α of R_g vs M is given in the caption of Fig. 2. The α values for random coils are between 0.5 and 0.6 for many polymers in good solvent, and a smaller α value than the range hints the presence of long-chain branches (Davidson et al. 1987; Grcev et al. 2004; Sun et al. 2001; Wyatt 1993). For PP-A, α value of 0.55 is obtained, which is a typical value for a random coil in a solvent and close to the theoretical exponent of 0.588 (Guillou and Zinn-Justin 1977). This suggests that PP-A takes random coil conformation in the solvent. The α values of PP-B and C are 0.43 and 0.46, respectively, and smaller than that of PP-A, implying that the degree of branching of PP-B and C is enough to affect their R_g to appreciable extent in the solution.

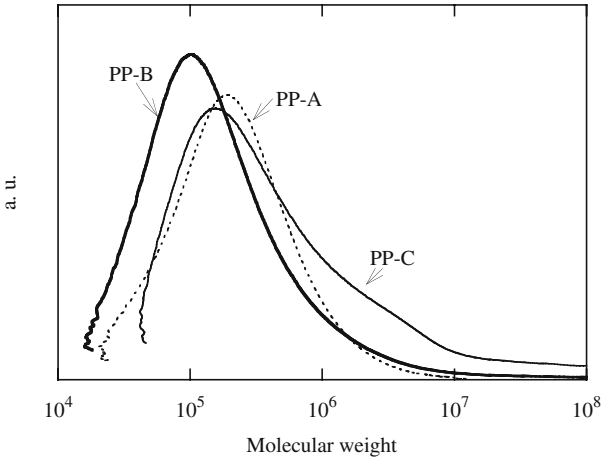

Fig. 1 Molecular weight distribution of PP-A, PP-B, and PP-C

GPC-MALLS technique provides another important branching characteristic which can be calculated as the number of branches per molecules. The relation between the branching number per molecule and g parameter depends on the branching functionality and the polydispersity of the sample. We assumed that PP-B and PP-C contain tri-functional random branch architecture. For the tri-functional random branch polymer, it is known for polydispersed polymer that g (Zimm and Stockmayer 1949) can be expressed in terms of the number of branches per molecule m as

$$g = \frac{6}{m}\left\{\frac{1}{2}\left(\frac{2+m}{m}\right)^{1/2} ln\left[\frac{(2+m)^{1/2}+m^{1/2}}{(2+m)^{1/2}-m^{1/2}}\right] - 1\right\} \tag{3}$$

We used Eq. (4) to calculate the degree of branching per molecule for each narrow fraction eluted from a GPC columns. The long-chain branching frequently λ can be calculated from the number of branches and defined as the number of branches per 1,000 repeat units,

$$\lambda = 1,000w\frac{m}{M} \tag{4}$$

where w is molecular weight of monomer unit. Finally, a practical issue should be mentioned here. To obtain a value of g from the experimental radius of gyration data of linear and branched polymer (see Eq. (1)), the molecular weight of both polymers should be the same. The degree of branching g can only be calculated for overlapped section of the molecular weights for linear and branched polymers. We calculated the values of the radii of gyration in high molecular weight region (10^7–10^8 for PP-A, $10^{7.5}$–10^8 for PP-B and PP-C) by extrapolation of each linear part of semilogarithmic plots, supposing that the linear relationship held even in the high molecular weight region. Fig. 3 shows the branching frequency calculated from Eq. (4) as a function of molecular weight for PP-B and PP-C. The long-chain branching frequency λ of PP-B decreased with an increase in molecular weight. λ for PP-C showed relatively gradual decrease with molecular weight (less than $10^{7.5}$). What has to be noticed is an increase in λ with 8 molecular

Table 1 Molecular and thermal characterization of samples

Code	MFR (g/10 min)	$\overline{M}n(10^{-5})$	$\overline{M}w(10^{-5})$	$\overline{M}w/\overline{M}z$	T_m (°C)	a_T (kJ/mol)
PP-A	3.5	1.3	3.9	3.0	160.4	37
PP-B	4.4	0.8	5.4	7.0	154.3	42
PP-C	3.0	1.6	15.8	9.6	156.9	48

PP-A, PP-B, PP-C polypropylene (grades A, B, and C, respectively), *MFR* melt flow rate

weight in the fairly high molecular weight range. This suggests a presence of highly branched chains with high molecular weights, though the values in the high molecular weight region may be argued due to its assumption which was mentioned before.

Table 1 shows the results of melting temperature T_m measurements. In the DSC thermograms, all the samples showed a single endotherm peak and monomodal curves. PP-B and PP-C, which have broad molecular weights, indicate lower T_m's than that of PP-A.

Dynamic tests: small amplitude oscillatory shear

Thermal stabilities of the samples were confirmed by time-sweep tests under constant angular frequency (ω=0.1 rad/s) and temperatures (180, 190, 200, and 210°C). Each dynamic test was carried out within the stable durations of the samples. The dynamic measurements are carried out at 180, 190, and 210°C. The results were horizontally shifted to the curve at 180°C of the reference temperature. The principle of time-temperature superposition was valid for all the samples. Figs. 4, 5 and 6 show the storage modulus G' and the loss modulus G'' plotted as a function of angular frequencies at a reference temperature of 180°C for PP-A to PP-C. The shear viscoelasticity behavior of PP-A is typical for that reported by many researchers, though the terminal flow regime where G' and G'' are proportional to ω^2 and ω, respectively, is not observed within this frequency region. At low frequencies, the deformation is more viscous than elastic for most uncross-linked polymers; G'' is greater than G'. Note that, on the other hand, Figs. 5 and 6 exhibit that values of G' and G'' of PP-B and PP-C are parallel to each other over a wide frequencies tested here. The melt rheology is used in the determination of the gel point for thermosetting and cross-linkable polymers. At a transition near the gel point of stoichiometrically balanced networks, G' and G'' show crossover values over a wide range of frequencies. The gel point appears in deficient cross-linker system when G' and G'' are parallel to each other. The gel point characterization method developed by Chambon and Winter (1987, 1986) has been used to define the exact point of conversion from liquid to solid, a chemical network with permanent cross-links. According to this criterion, this gel point is defined as the point at which the moduli scale in an identical fashion with frequency,

$$G'(\omega),\ G''(\omega) \sim \omega^n \quad 0 < n < 1 \tag{5}$$

or

$$G''(\omega)/G'(\omega) = tan(n\pi/2) \tag{6}$$

where n is called the relaxation exponent and can be linked to microstructural parameter. The frequency independency

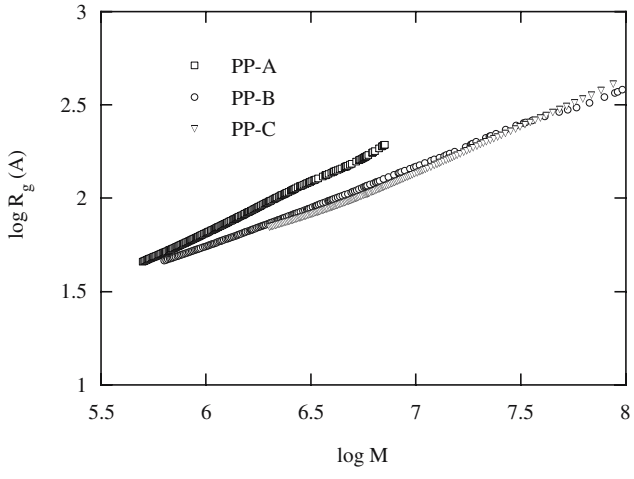

Fig. 2 Root mean square radius as a function of molecular weight of PP-A, PP-B, and PP-C. Slopes of the conformational plots are 0.55, 0.43, and 0.46, respectively

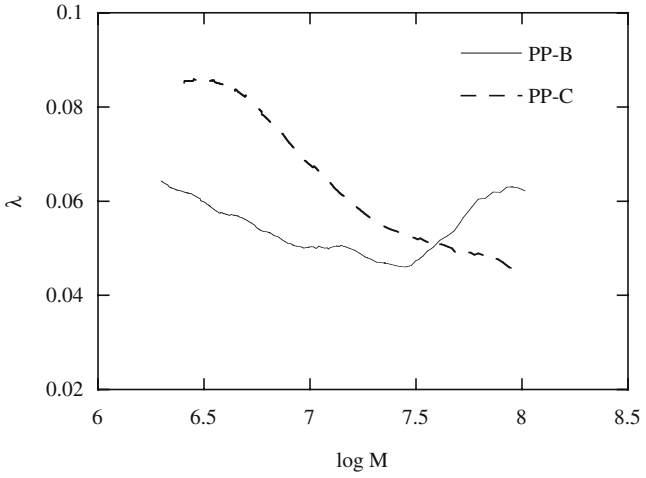

Fig. 3 Branching degree of PP-B and PP-C

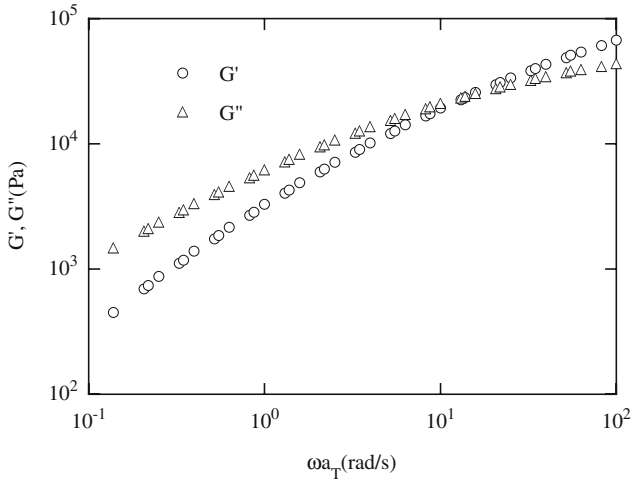

Fig. 4 G' and G'' curves of PP-A plotted as a function of angular frequencies at 180°C

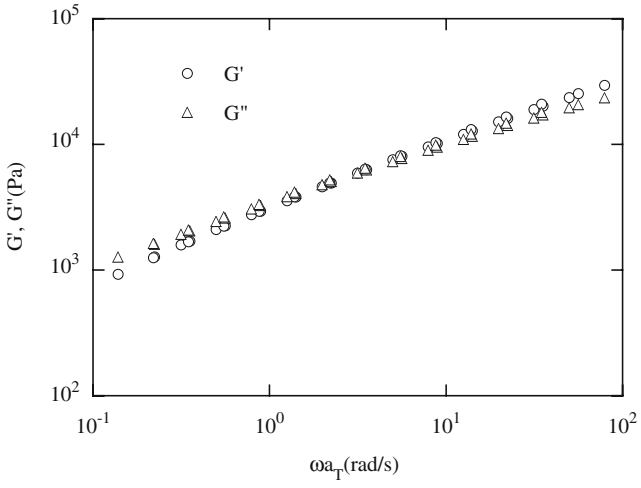

Fig. 6 G' and G'' curves of PP-C plotted as a function of angular frequencies at 180°C

of loss tangent tan $\delta(G''/G')$ has been widely examined for chemical and physical gels (Chambon and Winter 1987; Chiou et al. 2001; Li and Aoki 1997; Power and Rodd 1998; Winter and Chambon 1986). Fig. 7 indicates tan δ as a function of frequencies for PP-A, PP-B, and PP-C. The result, i.e., tan δ independency on frequency, implies that the melt rheological behaviors of PP-B and PP-C corespond to that of cross-linked polymer in the gel point according to Eqs. (5) and (6). Furthermore, the exponent n is found to be 0.46 (PP-B) to 0.53 (PP-C) for G' and G'' from Figs. 5 and 6. Chambon et al. (1986) and Chambon and Winter (1987) reported that n was found to be 0.5 and independent of the strand length between cross-links for stoichiometrically balanced, difunctional, endlinking polyurethanes and polydimethylsiloxanes. The low specific exponent value of n (~0) indicates a rigid gel, while the exponent approaching 1 indicates a more viscous gel. In general, excess cross-linker gives rise to a generation of three-dimensional chemical gel, and deficient cross-linker results in poor processability in polymer fabrication. From mentioned above, it is possible that PP-B and PP-C were prepared at balanced stoichiometry in consequence.

The horizontal shift factors a_T of all the samples were obtained by small oscillation measurements. Then the activation energies E_v's of flow were calculated by an Arrhenius plot of the shift factor against the reciprocal of the absolute temperature. The E_v values of PP-A, PP-B, and PP-C are shown in Table 1. E_v of PP-A is almost the same as that reported for linear PP (Kurzbeck et al. 1999; Sugimoto et al. 2001a,b). E_v's of PP-B and PP-C are higher than that of PP-A. The high E_v can be related to molecular architecture such as long-chain branching or a (partially)

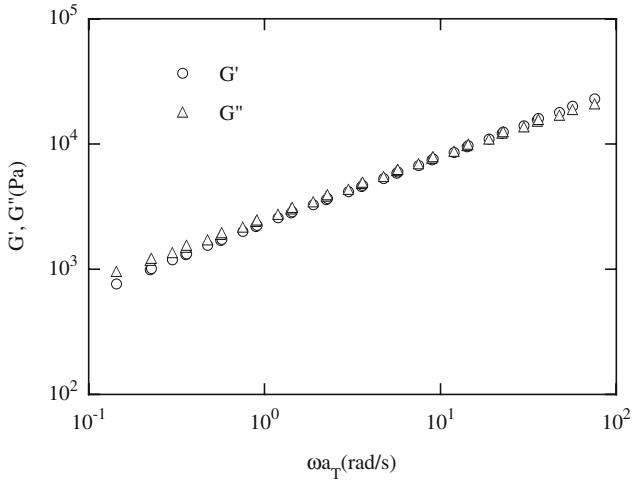

Fig. 5 G' and G'' curves of PP-B plotted as a function of angular frequencies at 180°C

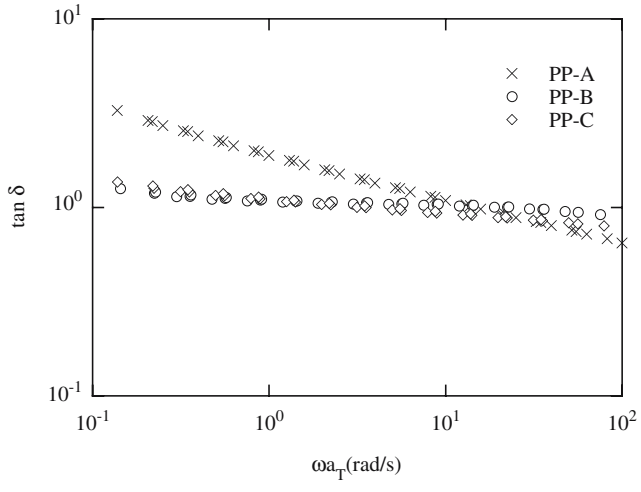

Fig. 7 tan δ curves of PP-A, PP-B, and PP-C plotted as a function of angular frequencies at 180°C

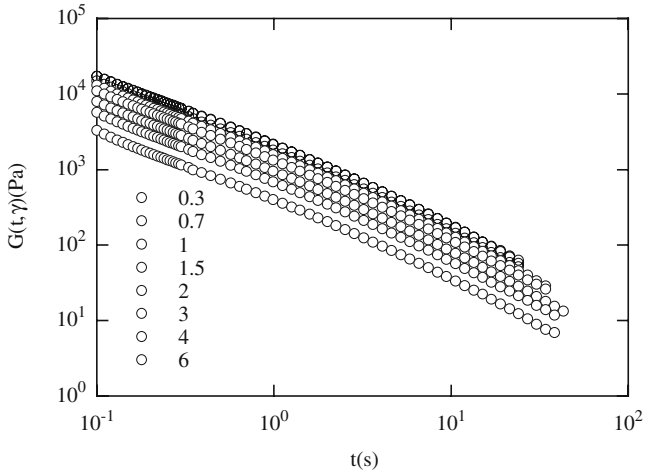

Fig. 8 $G(t, \gamma)$ of PP-A at 180°C for various strains 0.3, 0.7, 1, 1.5, 2, 3, 4, and 6, from *top* to *bottom*

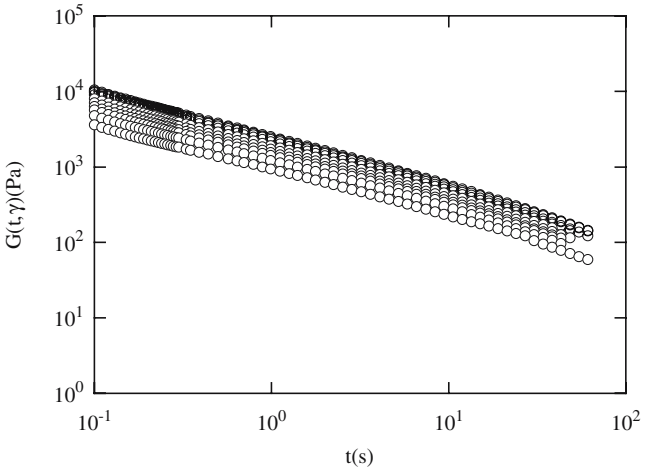

Fig. 10 $G(t, \gamma)$ of PP-C at 180°C for various strains 0.3, 0.5, 0.7, 1, 1.5, 2, 2.5, 3, 4, and 6, from *top* to *bottom*

cross-linked structure (Kurzbeck et al. 1999). Thus, the result implies that PP-C with higher E_v than that of PP-B has relatively high branching structure.

Step-shear stress relaxation

In the past, extensive studies were reported on the measurements of stress relaxation modulus of polymer solution and melts with flexible chains by imposing a sudden step strain (Archer 1999; Einaga et al. 1971; Fukuda et al. 1975; Inoue et al. 2002; Larson et al. 1988; Mhetar and Archer 2000; Osaki 1993; Osaki and Kurata 1980; Vrentas and Graessley 1982).

Figures 8, 9 and 10 show the time-dependent shear modulus, $G(t, \gamma)$, measured mechanically for PP-A to PP-C at various strains and constant temperature 180°C. As expected, the result of PP-A is similar to that of PP reported already, monotonically decreasing with time. For PP-C, we found from double-logarithmic plots of $G(t, \gamma)$ as a function of time that the shear relaxation modulus curves are parallel to each other. On the other hand, $G(t, \gamma)$ of PP-B curves seem to be not parallel to each other for different values of γ. The reproducibility or reliability of the data was carefully inspected by using other rheometer. This cannot be related to the experimental error such as malfunction of the rheometer and slippage at the wall. We shall discuss this unusual behavior of PP-B later.

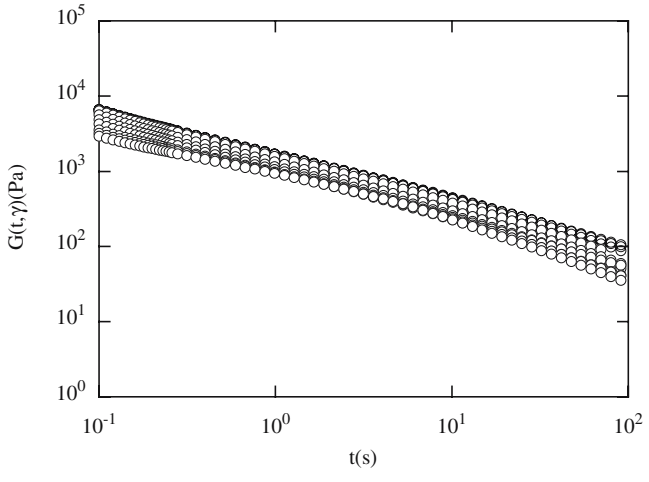

Fig. 9 $G(t, \gamma)$ of PP-B at 180°C for various strains 0.1, 0.2, 0.3, 0.5, 0.7, 1, 1.5, 2, 3, 4 and 5, from *top* to *bottom*

Elongational viscosity

The elongational viscosity $\eta_E^+\left(t, \dot{\varepsilon}\right)$ measurements were conducted by Meissner's elongational rheometer, which is described elsewhere (Ivanov et al. 2004; Kotaka et al. 1997; Meissner and Hostettler 1994; Schweizer 2000). The results of $\eta_E^+\left(t, \dot{\varepsilon}\right)$ on the three PPs are given in Fig. 11. The solid lines in the figure indicate three times linear viscosity $3\eta^+(t)$. The comparison of elongational viscosity growth function to $3\eta^+(t)$ corresponding to dynamic shear amplitude provides a check of validation of the data. $\eta_E^+\left(t, \dot{\varepsilon}\right)$ curves of PP-A overlap with $3\eta^+(t)$ at all the strain rates conducted, as expected from the theory of linear viscoelasticity (Trouton 1906). Likewise, $\eta_E^+\left(t, \dot{\varepsilon}\right)$ curves of PP-B and PP-C smoothly increase, and we confirmed the consistency of $\eta_E^+\left(t, \dot{\varepsilon}\right)$ with $3\eta^+(t)$ at shorter times, except slow rates data of PP-B (this is due to limited frequency range). At longer times, a pronounced increase in the elongational viscosity with time, so-called strain hardening, is found for these two samples at any strain rates. Even at the

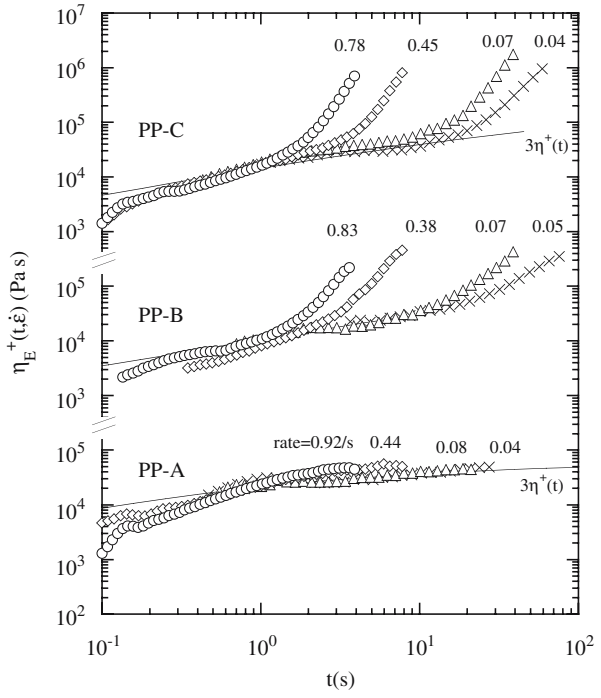

Fig. 11 Transient elongational viscosities of PP-A, PP-B, and PP-C at constant strain rates and temperature of 180°C. The *solid lines* indicate three times the dynamic viscosities, $3\eta^+$, at 180°C

smallest experimentally available value of $\dot{\varepsilon} = 0.05\ s^{-1}$, PP-B and PP-C show the strong upward deviations (the elongational viscosities increase by 2 orders of magnitudes). This is an unexpected behavior for conventional linear PP. The elongational viscosity of polymer melts is very sensitive to a presence of long-chain-branched molecules owing to its very long relaxation time. This has been shown in several polymers (Gotsis and Zeevenhoven 2004; Ogura and Takahashi 2003; Sugimoto et al. 1999; Wagner 2004), particularly in PE (Cogswell 1981; Dealy and Wissbrum 1990; Gabriel and Munstedt 2003; Munstedt et al. 1998; Schlund and Utracki 1987). The differences in the elongational behaviors, between high-pressure low-density PE with long-chain branches and linear one which shows much less strain hardening, have been extensively studied. We carried out calculations of the relaxation spectrum of PP-A, PP-B, and PP-C. The relaxation spectrum derived from the dynamic small amplitude tests was, however, incomplete for PP-B and PP-C because of the instability to reach very low frequencies in the experiments. In other words, either long times or high temperatures to estimate enough long relaxation time modes give rise to a degradation of the samples. As described before, Figs. 2 and 3 clearly indicate that PP-B and PP-C contain long-chain branches. The values of M_z show that the high molecular weight fraction is present in PP-B and PP-C. It seems reasonable to suppose that this high molecular weight tail is responsible for the observed strain hardening.

To allow quantitative analysis of the strain hardening behavior of the PPs, a parameter to represent the strain hardening may be defined by the ratio of $\eta_E^+\left(t, \dot{\varepsilon}\right)$ to $3\eta^+(t)$ (Sugimoto et al. 2001a,b). The ratio provides the intensity of the strain hardening. It is, however, difficult to compare the strain rate dependency of the parameter of PP-B and PP-C since $3\eta^+(t)$ curve range of PP-B is shorter than the elongation time due to the limited thermal exposure.

Chain structure of branched PP

The branched PPs, PP-B, and PP-C showed similar rheological response under shear and elongational flows. To further discuss the difference of the samples, the damping function derived from step-strain measurements and LAOS was employed.

Damping function

It is important to note the dependence of the nonlinear relaxation modulus on strain. The stress relaxation experiments have been used to provide a useful and convenient method for constitutive equations of viscoelastic fluids (Archer 1999; Inoue et al. 2002; Kasehagen and Macosko 1998; Osaki 1993; Osaki et al. 1996). Recently, a number of studies have been made on the nonlinear modulus to investigate the process of retraction along the tube of a chain extended by a large deformation. A lot of measurements on a variety of polymer liquids suggest that the nonlinear feature of $G(t, \gamma)$ for an entangled flexible polymer can be expressed in a factored form, over a certain time τ_k that depends on the system,

$$G(t, \gamma) = G(t)h(\gamma) \quad (t > \tau_k) \tag{7}$$

Here $G(t)$ is time-dependent shear modulus at small strain amplitude γ and is independent of strain and a unique function for a given polymer; $G(t)=\sigma(t)/\gamma$. $h(\gamma)$ is strain-dependent damping function, which represents how the stress is lower than the linear viscoelasticy limit. It has known that $h(\gamma)$ is a universal function and is accord with a value predicted by Doi-Edwards tube theory (Doi and Edwards 1986). It is clear from Figs. 8 and 10 that $G(t, \gamma)/G(t)$ obtained by the step-shear tests for PP-A and PP-C is constant at each strain. The ratios are very close to unity at small strains and level off with increasing strain. The values at each strain are essentially independent of time. This represents that the factorability of Eq. (7) is significantly valid for PP-A and PP-C as with those of various polymers. What has to be noticed is unusual step-shear behaviors of PP-B by an imposition of large strains. $G(t, \gamma)$ curves against γ for PP-B are not parallel to each

other (see Fig. 9). This can be more clearly explained by plotting $G(t, \gamma)/G(t)$ against time for various γ, as shown in Fig. 12. At small strains ($\gamma \leq 0.2$), $G(t, \gamma)/G(t)$ is independent of time, irrespective of the imposed strain. The curves of PP-B at large strains are, however, not to be simply translated along the vertical axis. At strains ranging from 0.3 to 1.5, the normalized curves monotonically decrease with time. Then, $\gamma \geq 3$, the curves initially increase with time until a peak is reached at a certain time but, after some time, manifest a gradual decrease. This tendency is more evident at large strains. Hence, the factorability expressed by Eq. (7) is not applicable to PP-B in the time scale done here.

Figure 13 shows time-dependent damping function $h(t, \gamma)$ calculated from the values at several discrete times for PP-B and $h(\gamma)$ for PP-A and PP-C. The dotted line through the data represents the damping function predicted by Doi and Edwards for linear and narrow molecular weight distribution polymer liquids. $h(\gamma)$ indicates a slightly weaker dependence on strain than the theoretical line. We may say that this is due to the polydispersity of the molecular weight. Furthermore, it has been known that a presence of long-chain branches brings about weaker strain dependence in $h(\gamma)$ (Kasehagen and Macosko 1998). In the case of PP-C, we consider that both factors result in the weaker dependence on strain than that of PP-A. As expected from Fig. 12, $h(t, \gamma)$ of PP-B is a time-dependent function and shows no sign of convergence of the curves to a damping function, irrespective of time, within the times tested in this study. Recently, Sanchez-Reyes and Archer (2002) and Islam et al. (2003) performed a detailed study on the nonlinear dynamics of entangled polymer solutions with ultrahigh molecular weight. They found that the factorability time (at which Eq. (7) can be applicable) is much longer than that of the longest Rouse relaxation time and more closely aligns with the terminal relaxation time, while the single damping function corresponds to the universal damping function predicted by Doi-Edwards theory beyond the factorability time. In our study, it is, however, difficult to discuss the unusual step-shear behaviors by correlating with the characteristic relaxation time owing to polydispersity and longer terminal relaxation time than time scale observed. Although the issue discussed here is still an open question, one possible explanation could be some extremely long relaxation mode or structure such as partial cross-link.

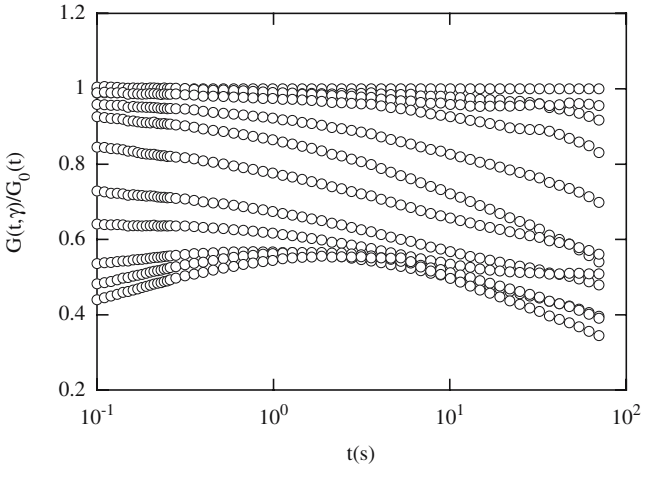

Fig. 12 *G(t, γ)/G(t)* against time for various shear strains at 180°C for PP-B

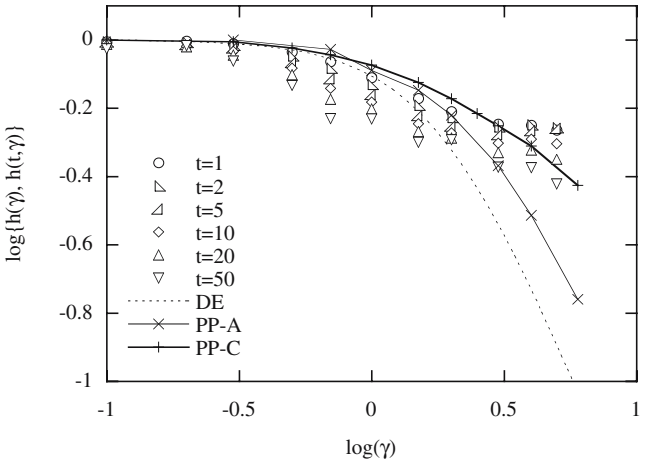

Fig. 13 Damping function $h(\gamma)$ for PP-A and PP-C, and time-dependent damping function $h(t, \gamma)$ for PP-B at various shear strains at 180°C. The *dashed line*, DE, is the damping function predicted by the Doi and Edwards theory[55]

Large amplitude oscillatory shear

The large amplitude oscillatory shear (LAOS) measurement was carried out for PP-A, PP-B, and PP-C. The LAOS test is a useful characterization method of viscoelastic fluids because strain amplitude and frequency can be varied independently allowing a broad spectrum of conditions to be attained (Yosick et al. 1997). Moreover, it is relatively easy to generate because oscillatory shear does not involve any sudden jump in speed or position (Giacomin and Dealy 1993). Hyun et al. (2002, 2003) have reported through dynamic strain sweep tests of various solutions that the nonlinear rheology provides more abundant information on the microstructure of a complex fluid, and the LAOS behaviors can be used as a way to classify complex fluids. LAOS test has, however, one disadvantage; the stress output is not simply sinusoidal any more at higher harmonic contributions (Dealy and Wissbrum 1990). When strain amplitude is large, the stress is no longer sinusoidal and has higher harmonic contributions,

$$\sigma(t) = \sum_{n=1,odd} \sigma_n sin(n\omega_1 t + \phi_n) \tag{8}$$

where the magnitude σ_n and the phase angle ϕ_n depend on strain amplitude and imposed frequency ω_1 (Giacomin and Dealy 1993). This disadvantage complicates the interpretation of data from large amplitude oscillatory tests. The algorithms to calculate G' and G'' from the stress signal generated by a rheometer cannot discriminate linear and nonlinear responses and will produce values for these functions even if the stress is sinusoidal. Thus, we need to investigate the stress data more precisely and systematically. There are two methods to analyze stress data at large strain amplitude; one is to investigate the stress shape directly, e.g., by Lissajours pattern (strain vs stress), and the other is the Fourier transformation method. Recently, to analyze higher harmonic contributions in LAOS, "high-sensitivity Fourier transformation rheology" method has been introduced by Wilhelm and co-workers (Wilhelm 2002; Wilhelm et al. 1998, 1999, 2000).

The strain sweep tests were conducted at 180°C. The linear regime in which the moduli are independent of strain amplitude was observed for all the samples in the small strain region. As strain is increasing, a decrease in both G' and G'', i.e., a strain thinning, was observed. This behavior is most typically observed for polymer solutions and melts as well as the shear thinning. The stress curves at 719% of strain are plotted in Fig. 14. What has to be noticed is their different stress patterns observed here, though the materials showed similar strain thinning behavior. PP-A shows the "forward tilted" shape. On the other hand, PP-B and PP-C show the "backward tilted" shape (Hyun et al. 2003). The origin of "forward tilted" shoulder may be the alignment of polymer chains with the flow direction. For PP-B and PP-C, we may say that nonlinear structure such as branching plays a role as a resistance or as an obstacle for the alignment of polymer chains to the flow direction, which makes the samples show the "backward tilted" stress shape.

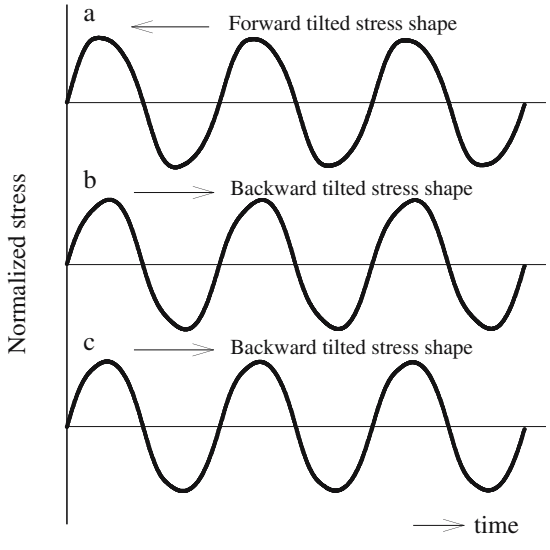

Fig. 14 Normalized stress plotted against time at angular frequency 1 rad/s, constant strain amplitude 719%, and temperature 180°C for PP-A (**a**), PP-B (**b**), and PP-C (**c**)

It is important and interesting to quantify the degree of nonlinear response under large strain by the ratio of the higher harmonic intensity to the first harmonic intensity. It has been reported that the higher harmonics increases as the imposed strain increases for polymer solutions such as aqueous xanthan gam, poly(vinyl alcohol), hyaluronic acid, polystyrene, polyisobutylene solutions, and polymer dispersions in water and atactic PP melt. Only few attempts have so far been made at long-chain-branched polymer melts, though the Fourier transformation analysis is one of the useful means to consider in the complex microstructure. More study on LAOS will be needed to get the total picture since little is understood on the physical significance of the higher harmonic contributions of stress intensity and phase angle. The results will be reported elsewhere in the future.

Concluding remarks

We found that even an extremely small amount of 1,9-decadiene incorporation to PP had a great influence on the molecular architecture and the rheological behaviors, though the diene components were not detected by NMR. MFR of the propylene/1,9-decadiene copolymer strongly depended on the concentration of diene monomer. An incorporation of small fraction of diene monomer clearly increased the molecular weight and molecular weight distribution. From GPC-MALLS analysis, PP-C showed extensive tail in the high molecular weight region, while PP-B did not show appreciable change in the high molecular weight tail in comparison with PP-A. MALLS exhibited, however, a presence of a small amount of branching chains of PP-B and PP-C in the high molecular weight fractions. From the branching chain frequency analysis, it is possible that λ of PP-B has a small dependence on the molecular weight and large value in the high molecular weight fraction. Both branched PPs showed an increase in the extremely long relaxation mode at rheological characterizations: apparently enhanced elasticity, strong non-Newtonian behavior, and gradual decline of relaxation modulus under shear flow. In addition, PP-B copolymerized with an extremely small amount of diene showed the outstanding strain hardening under elongational flow, as well as PP-C, which is unexpected for linear conventional PP. However, under step-strain flow, PP-B indicated that $G(t, \gamma)$ curves at various γ were not parallel to each other and not factorable into two functions within the tested time. The nonfactorable damping function is unusual for entangled flexible polymers. We consider that this rheological behavior implies a presence of microstructure that causes the unusual relaxation mode. The LAOS experiments provided some interesting results from stress intensity and phase angle. The branched PPs showed "backward tilted shoulder" stress signal, while linear PP showed "forward tilted shoulder." We consider that this is due to the alignment of polymer chains with the flow direction. The result of LAOS may lead a lot of useful information on the fluid microstructure by the high-sensitivity Fourier transformation method, related to the

polymer processing undergoing large deformation. It is, however, difficult to discuss it from the result of LAOS at present since the relationship between the contribution of higher harmonic and the microstructure is less well understood for long-chain-branched polymer. Further work will be needed to analyze the physical significance of the moduli in the nonlinear region.

Acknowledgements The authors would like to thank Chisso Corporation and Japan Polypropylene Corporation for providing samples. The authors are grateful to Mr. H. Shikuma, Shiga Industrial Support Plaza, for valuable suggestions and discussions. We thank Yonezawa Kogyo-kai of Yamagata University for their financial support.

References

Archer LA (1999) Separability criteria for entangled polymer liquids. J Rheol 43: 1555–1571

Chambon F, Winter HH (1987) Linear viscoelasticity at the gel point of a crosslinking PDMS with imbalanced stoichiometry. J Rheol 31:683–697

Chambon F, Petrovic ZS, MacKnight WJ, Winter HH (1986) Rheology of model polyurethanes at the gel point. Macromolecules 19: 2146–2149

Chiou B-S, Raghavan SR, Khan SA (2001) Effect of colloidal fillers on the crosslinking of a UV-curable polymer: gel point rheology and the Winter-Chambon criterion. Macromolecules 34:4526–4533

Cogswell FN (1981) Polymer melt rheology. Woodhead, Cambridge

Davidson NS, Fetters LJ, Funk WG, Hadjichristidis N, Graessley WW (1987) Measurement of chain dimensions in dilute polymer solutions: a light scattering and viscometric study of linear polyisoprene in cyclohexane. Macromolecules 20:2614–2619

Dealy JM, Wissbrum KF (1990) Melt rheology and its role in plastic processing: theory and applications. Van Nostrand, New York

Doi M, Edwards SF (1986) The theory of polymer dynamics. Oxford Science, New York

Einaga Y, Osaki K, Kurata M, Kimura S, Tamura M (1971) Stress relaxation of polymer solutions under large strain. Polym J 2:550–552

Fukuda M, Osaki K, Kurata M (1975) Nonlinear viscoelasticity of polystylene solutions. I. Strain-dependent relaxation modulus. J Polym Sci Polym Phys Ed 13:1563–1576

Gabriel C, Munstedt H (2003) Strain hardening of various polyolefins in uniaxial elongational flow. J Rheol 47:619–630

Gabriel C, Kokko E, Lofgren B, Seppala J, Munstedt H (2002) Analytical and rheological characterization of long-chain branched metallocene-catalyzed ethylene homopolymers. Polymer 43:6383–6390

Giacomin AJ, Dealy JM (1993) Large-amplitude oscillatory shear, techniques in rheological measurements. Chapman & Hall, London

Gotsis AD, Zeevenhoven BLF (2004) Effect of long branches on the rheology of polypropylene. J Rheol 48:895–914

Grcev S, Schoenmakers P, Iedema P (2004) Determination of molecular weight and size distribution and branching characteristics of PVAc by means of size exclusion chromatography/multi-angle laser light scattering (SEC-MALLS). Polymer 45:39–48

Guillou JCL, Zinn-Justin J (1977) Critical exponents for the n-vector model in three dimensions from field theory. J Phys Rev Lett 39:95–98

Hingmann R, Marczinke B (1994) Shear and elongational flow properties of polypropylene melts. J Rheol 38:573–587

Hyun K, Kim SH, Ahn KH, Lee SJ (2002) Large amplitude oscillatory shear as a way to classify the complex fluids. J Non-Newton Fluid Mech 107:51–65

Hyun K, Nam JG, Wilhelm M, Ahn KH, Lee SJ (2003) Nonlinear response of complex fluids under LAOS (large amplitude oscillatory shear) flow Korea-Australia. Rheol J 15:97–105

Inoue T, Yamashita Y, Osaki K (2002) Viscoelasticity of an entangled polymer solution with special attention on a characteristic time for nonlinear behavior. Macromolecules 35:1770–1775

Islam MT, Sanchez-Reyes J, Archer LA (2003) Step and steady shear responses of nearly monodisperse highly entangled 1,4-polybutadiene solutions. Rheol Acta 42:191–198

Ivanov I, Muke S, Kao N, Bhattacharya SN (2004) Extensional rheology of polypropylene in relation to processing characteristics. Int Polym Process 19:40–46

Kasehagen LJ, Macosko CW (1998) Nonlinear shear and extensional rheology of long-chain randomly branched polybutadiene. J Rheol 42:1303–1327

Kokko E, Pietikainen P, Koivunen J, Seppala JV (2001) Long-chain-branched polyethylene by the copolymerization of ethane and nonconjugated α,-dienes. J Polym Sci A Polym Chem 39:3805–3817

Kotaka T, Kojima A, Okamoto M (1997) Elongational flow opto-rheometry for polymer melts—1. Construction of an elongational flow opto-rheometer and some preliminary results. Rheol Acta 36:646–656

Kurzbeck S, Oster F, Munstedt H, Nguyen TQ, Gensler R (1999) Rheological properties of two propylenes with different molecular structure. J Rheol 43:359–374

Larson RG, Khan SA, Raju VR (1988) Relaxation of stress and birefringence in polymers of high molecular weight. J Rheol 32:145–161

Li L, Aoki Y (1997) Rheological images of poly(vinyl chloride) gels. 1. The dependence of sol-gel transition on concentration. Macromolecules 30:7835–7841

Meissner J, Hostettler J (1994) A new elongational rheometer for polymer melts and other highly viscoelastic liquids. Rheol Acta 33:1–21

Mhetar VR, Archer LA (2000) A new proposal for polymer dynamics in steady shearing flows. J Polym Sci B Polym Phys 38:222–233

Munstedt H, Kurzbeck S, Egersdorfer L (1998) Influence of molecular structure on rheological properties of polyethylenes. Rheol Acta 37:21–29

Ogura K, Takahashi M (2003) Uniaxial and biaxial behavior of a lightly cross-linked PMMA melt at constant rates. J Soc Rheol Jpn 31:79–83

Osaki K (1993) On the damping function of shear relaxation modulus for entangled polymers. Rheol Acta 32:429–437

Osaki K, Kurata M (1980) Experimental appraisal of the Doi-Edwards theory for polymer rheology based on the data for polystyrene solutions. Macromolecules 13:671–676

Osaki K, Watanabe H, Inoue T (1996) Damping function of the shear relaxation modulus and the chain retraction process of entangled polymers. Macromolecules 29:3611–3614

Paavola S, Saarinen T, Lofgren B, Pitkanen P (2004) Propylene copolymerization with non-conjugated dienes and α-orefins using metallocene catalyst. Polymer 45:2099–2110

Power DJ, Rodd AB (1998) Gel transition studies on nonideal polymer networks using small amplitude oscillatory rheometer. J Rheol 42:1021–1037

Sanchez-Reyes J, Archer LA (2002) Step shear dynamics of entangled polymer liquids. Macromolecules 35:5194–5202

Scheve BJ, Mayfield JW, Denicola AJ (1990) High melt strength, propylene polymer, process for making it, and use thereof. Himont Inc., US Patent 4,916,198

Schlund B, Utracki LA (1987) Polym Eng Sci 27:380

Schweizer T (2000) The uniaxial elongational rheometer RME—six years of experience. Rheol Acta 39:428–443

Soskey JF, Winter HH (1984) Large step shear strain experiments with parallel-disk rotational rheometers. J Rheol 28:625–645

Sugimoto M, Masubuchi Y, Takimoto J, Koyama K (1999) Effect of chain structure on the melt theology of modified polypropylene. J Appl Polym Sci 73:1493–1500

Sugimoto M, Masubuchi Y, Takimoto J, Koyama K (2001a) Melt rheology of polypropylene containing small amounts of high molecular weight chain. I. Shear flow. J Polym Sci Part B Polym Phys 39:2692–2704

Sugimoto M, Masubuchi Y, Takimoto J, Koyama K (2001b) Melt rheology of polypropylene containing small amounts of high-molecular-weight chain. 2. Uniaxial and biaxial extensional flow. Macromolecules 34:6056–6063

Sun T, Brant P, Chance RR, Graessley WW (2001) Effect of short chain branching on the coil dimensions of polyorefins in dilute solution. Macromolecules 34:6812–6820

Trouton FT (1906) On the coefficient of viscous traction and its relation to that of viscosity. Proc R Soc Lond A Math Phys Sci 77:426–440

Tsenoglou CJ, Gotsis AD (2001) Rheological characterization of long chain branching in a melt of evolving molecular architecture. Macromolecules 34:4685–4687

Tsutsui M, Maehara H, Hatada K, Ushioda T (2001) Polypropylene base resin composition for foam-molding, foamed article using the same composition, production process for the same foamed article and foam-molded product using the foamed-article. Chisso Co., US Patent 2001/0020045 A1

Vrentas CM, Graessley WW (1982) Study of shear stress relaxation in well-characterized polymer liquids. J Rheol 26:359–371

Wagner MH (2004) Relating rheology and molecular structure of model branched polystyrene melts by molecular stress function theory. J Rheol 48:489–503

Weng W, Hu W, Dekmezian AH, Ruff CJ (2002) Long chain branched isotactic polypropylene. Macromolecules 35:3838–3843

Wilhelm M (2002) Fourier-transform rheology. Macromol Mater Eng 287:83–105

Wilhelm M, Maring D, Spiess H-W (1998) Fourier-transform rheology. Rheol Acta 37:399–405

Wilhelm M, Reinheimer P, Ortseifer M (1999) High sensitivity Fourier-transform rheology. Rheol Acta 38:349–356

Wilhelm M, Reinheimer P, Ortseifer M, Neidhofer T, Spiess H-W (2000) The crossover between linear and non-linear mechanical behavior in polymer solutions as detected by Fourier-transform rheology. Rheol Acta 39:241–246

Williams SD, Yoo HJ, Drickman MR (1998) Radiation visbroken polypropylene and fibers made therefrom. US Patent 5,820,981

Winter HH, Chambon F (1986) Analysis of linear viscoelasticity of a crosslinking at the gel point. J Rheol 30:367–382

Wong B, Baker WE (1997) Melt rheology of graft modified polypropylene. Polymer 38:2781–2789

Wyatt PJ (1993) Light scattering and the absolute characterization of macromolecules. Anal Chim Acta 272:1–40

Ye Z, AlObaidi F, Zhu S (2004) Synthesis and rheological properties of long-chain-branched isotactic polypropylenes prepared by copolymerization of propylene and nonconjugated dienes. Ind Eng Chem Res 43:2860–2870

Yoshii F, Makuuchi K, Kikukawa S, Tanaka T, Saitoh J, Koyama K (1996) High-melt-strength polypropylene with electron beam irradiation in the presence of polyfunctional monomers. J Appl Polym Sci 60:617–623

Yosick JA, Giacomin AJ, Moldenaers P (1997) A kinetic network model for nonlinear flow behavior of molten plastics in both shear and extension. J Non-Newton Fluid Mech 70:103–123

Zimm BH, Stockmayer WH (1949) The dimensions of chain molecules containing branches and rings. J Chem Phys 17:1301–1314